

Filled Thermoconductive Plastics for Fused Filament Fabrication

T. Mulholland¹, A. Falke², N. Rudolph¹

1. Department of Mechanical Engineering, University of Wisconsin, Madison, WI 53706

2. RWTH Aachen University, North Rhine-Westphalia, Germany

Abstract

Although thermoplastics have traditionally been ignored as heat transfer materials, filled thermally conductive plastics fabricated in complex geometries can serve as low-cost, geometrically complicated heat exchangers, along with other thermal applications such as heat sinks. Thermally conductive, 3D printed heat exchangers can have a significant impact on power generation technology at many scales, with advantages in allowing distributed, on-site manufacturing on multiple, independent machines, and the virtual elimination of scrap. This can command significant cost savings compared to traditional, machined metal heat exchangers. This work examines compounds of polyamide 6 with copper fiber and sphere fillers produced in a co-rotating twin screw extruder. The thermal conductivity is measured and related to the filler content, shape, and orientation.

Keywords: 3D Printing, FFF, Thermal Conductivity

Introduction

Despite a wide variety of manufacturing processes and a growing list of suitable materials, additive manufacturing (AM) has traditionally been regarded as a rapid prototyping technique. Several obstacles remain for producing competitive, functional parts.

Two major barriers are the anisotropy and weld line formation introduced by the layer-upon-layer processes and their effect on the mechanical properties. This can be seen in studies of build orientation [1-8] and bead orientation [1-3, 5, 6, 9-13]. The part strength is higher in cases where the load is applied in the in-plane direction since it depends on the material itself, and the strength is lower when the load is applied in the build direction since the strength reflects the bonding between layers. Notably, recent studies suggest that the orientation of the individual beads in a part produced by Fused Filament Fabrication may permit strengths almost as high as an injection molded part, if the printed part is sufficiently dense [14]. Fused filament fabrication (FFF), otherwise known by the trademarked name fused deposition modeling (FDMTM), is a widely known and easily accessible AM technique with a huge potential for functionality growth, given the essentially limitless choices of possible materials. However, commercial functional materials are only now starting to enter the market.

AM already excels at creating parts with traditionally-impossible, complex geometries, and the potential uses of the technology will continue to grow along with the material choices. The effects of orientation are important for other material properties besides the mechanical strength. Oriented conductivity in AM parts could be a boon for the AM sector in both electrical and thermal applications.

There are many applications that could benefit from oriented conductivity, from electrical conductors and circuits to thermal applications and heat fins. Importantly, in most of these cases the mechanical strength is less important than other properties. Thus, these applications can serve as a platform from which to grow industrial use of AM technologies, where AM parts can directly compete with traditional manufactured parts.

Since polymers have a very low conductivity, filler particles must be added to achieve enhanced thermal or electrical conductivity. The orientation of filler materials in plastic resins during injection molding is known to have a strong influence on the thermal conductivity, and to be a direct result of the manufacturing method [15, 16]. The most important factors influencing thermal conductivity in filled plastics are the filler content, size, and shape. Thermal conductivity is best enhanced when continuous pathways are chained through the part via contact between the filler particles [17]. The combination of continuous pathways and oriented conductivity suggest that suitable particles should have a high aspect ratio, for example fibers, and that the filler must be added at relatively high volume fractions. For filled FFF filament, early work by Gray et al. [18, 19] demonstrated increased mechanical performance by reinforcing polypropylene with liquid crystalline polymer (LCP) fibrils. Zhong et al. [20] prepared a glass fiber filled ABS filament for a commercial FFF printer. Although improved strength was achieved, plasticizer and compatibilizer were added to realize the flexibility and handleability needed for processing. Masood and coworkers developed a metal-polymer filament designed for rapid tooling of injection molding inserts [21, 22]. Iron powder (200-500 μm) with volume fractions of up to 40% was added to a polyamide matrix to make FLM filament feedstock capable of processing through a commercial FFF system. In 2012 the first electrical conductive FFF filament was produced with 15 % wt carbon black to print several flexible sensors and capacitive buttons [23]. The same year, Oak Ridge National Laboratory (ORNL) demonstrated printing with short fiber feedstock in public [24] and evaluated the mechanical properties of printed parts [25]. Protoplant Inc., Vancouver, WA, (www.protoplant.com) and the Kickstarter company Functionalize (www.functionalize.com) recently introduced a carbon black or graphite filled filament for the desktop-printer market for increased thermal and electrical conductivity. To make FFF filament with increased thermal conductivity a viable printing option, an understanding of the complex interaction between matrix and fillers needs to be established, which is dependent on the material properties, the filler size, shape and orientation as well as the manufacturing processes (compounding, extrusion, printing) involved.

This work aims to provide a foundation for developing materials useful for fabricating air-to-water heat exchangers produced via FFF. Complicated geometries can be produced via FFF at little added cost, which allows in this case the manufacture of pin fin heat exchangers with complex pin shapes, such as tapered ellipses and air foils. This easily permits the plastic-based heat exchangers to surpass traditional metal heat exchangers with only modest increases in the base material thermal conductivity. It is worth noting that, due to the high convective resistance associated with the air side of the heat exchanger, the material thermal conductivity only needs to be raised to modest values to make an effective heat exchanger. Additionally, the orientation of shaped fillers along the pin axis can significantly increase the heat exchanger performance [26].

In order to be able to tailor thermal properties for any application, it is important to find an accurate way to measure thermally conductive filament. This can be challenging, since even the sample preparation can alter the filler orientation, leading to changes in the thermal conductivity. This article outlines the steps taken to produce filled materials for use in FFF, as well as to analyze the effects of filler type and orientation.

Methods

Material

Polyamide 6 (PA6), sometimes referred to by the original trade name Nylon, was chosen for this study because of its high heat resistance and mechanical properties. Ultramid B33-01 (BASF, Germany) with a melting temperature of 220 °C and a density of 1.13 g/cm³ was used. The moisture content at 50 % relative humidity is 2.6 %. Similar PA6 grades from BASF report thermal conductivity and specific heat capacity values of 0.33 W/m-K and 1500 – 1700 J/kg-K, respectively.

The material has an intermediate viscosity, which is important for FFF material production. For filament production, a relatively high viscosity is preferable to aid in molten material handling during line startup. In contrast, FFF machines require a relatively low viscosity, due to the low pressures that can be generated in these devices. Additionally, the use of fillers will increase the viscosity. Thus, an intermediate viscosity PA6 is the preferable choice for mixing with the conductive fillers.

Spherical copper particles with a nominal diameter below 45 micrometers were purchased (Chemical Store, USA). The spheres are 99.5% copper, with a small iron content and a density of 8.9 g/cm³. They are produced via air atomization of molten copper. 99.9% of the spheres are smaller than 325 µm, with the other 0.1% falling in the range of 45 to 74 µm.

Copper fibers with a nominal diameter of 30 µm and a nominal length of 3 mm were purchased from Deutsches Metallfaserwerk (Germany). The fibers are a minimum 99.9% copper, with a density of 8.9 g/cm³ and a thermal conductivity of 383 W/m-K. To produce the fibers, copper strands are first made into a fleece, which is then chopped.

Material Compounding

The copper spheres and copper fibers were mixed separately into the PA6 using a twin screw compounding extruder with 27 mm intermeshing, co-rotating screws and a 36 diameter length (927 mm), manufactured by Leistritz Corp. (USA). Twin screw extruders are known to be superior for the mixing of highly filled systems when compared to traditional single screw extruders. Different elements of the fully-customizable screw set are used to melt the resin, generate pressure, and homogenize the melt temperature and filler distribution. The screw design, along with qualitative descriptions of the screw elements, is shown below in Figure 1.

While the PA6 pellets are supplied by a first gravimetric feeder to the extruder at the beginning of the screw, the filler is supplied by a second gravimetric feeder after the resin is melted using twin, intermeshing augers, aptly named the side stuffer. The degassing zone, near the end of the extruder, allows volatiles to escape the material before extrusion, including for

example volatile plasticizers, gaseous degradation products, or water vapor. The latter option is relevant for PA6 processing, since this material is very hygroscopic.

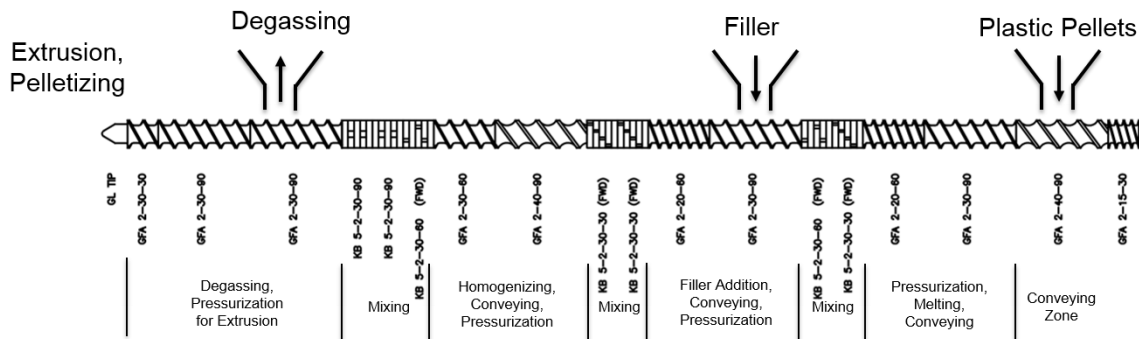


Figure 1. Screw design for compounding PA6 with copper spheres or fibers.

The parameters listed below in Table 1 were used to produce the copper filled PA6 materials. The copper spheres were produced with a flat temperature zone profile at 240 °C, which resulted in a melt temperature of 253 °C. The copper fiber filled PA6 was produced with a steady temperature zone ramp from 220 to 240 °C, with a melt temperature around 240 °C. The extruder screw speed was 100 RPM, and the side stuffer speed was 140 RPM.

Table 1. Twin screw extruder parameters for copper fiber filled PA6.

Copper Fiber Volume Fraction	Melt Temperature	Resin Feed Rate	Filler Feed Rate	Total Mass Flow Rate	Puller Speed
20%	253 °C	6.7 kg/hr	13.3 kg/hr	20 kg/hr	11 m/min

The material was extruded through a three-strand die with an orifice diameter of 3.0 mm. The strands were pulled at a constant velocity by a precision belt puller (ConAir, USA). Uneven flow through the die, caused by uneven pressure distribution and gradual clogging of the orifices, caused differences in the material flow rate, which yielded strands of differing diameters. The strands were later classified as D1 (diameter range 1.1 to 1.76 mm), D2 (diameter range 1.8 to 2.4 mm), and D3 (2.44 to 3.3 mm). The different flow rates and the take-up by the belt puller led to natural differences in the fiber orientation, which were subsequently analyzed by different techniques.

Thermogravimetric Analysis (TGA)

The actual filler content was determined by thermogravimetric analysis (TGA) with a Netzsch TG 209 F1 Libra. In this technique, the sample, about 3 mg of polymer if unfilled, is heated at a constant rate in an inert gas atmosphere, in this case nitrogen, and the weight is constantly measured with a resolution of 0.1 µg. These samples were heated up to 600 °C at a rate of 20 K/min with a constant nitrogen flow of 20 mL/min. To exclude the weight of water in hygroscopic PA6, the initial weight of the compound was taken as the sample weight at 270 °C. The mass of the filler is taken as the sample weight at 600 °C. These two masses are used to directly calculate the mass fraction of filler, and the densities of each material can then be used to calculate the volume fraction of filler.

Laser Flash Analysis (LFA)

LFA is used to determine the thermal diffusivity of a sample. The instrument, a Nanoflash 447 from Netzsch Instruments (Germany), fires a xenon flash lamp at the bottom side of the sample, while a liquid-nitrogen cooled infrared detector monitors the top side of the sample. The diffusivity of the sample can then be calculated from only the sample thickness (L) and the half time ($t_{1/2}$) of the temperature rise on the top surface, according to the following [27]:

$$\alpha = \frac{1.38 L^2}{\pi^2 t_{1/2}} \quad (\text{Eq. 1})$$

Additional models are available to correct for certain errors. This work used the Cowan model [28], a standard choice that corrects for radiative or convective losses from the top and bottom surfaces of the sample, as well as a correction for the time of the energy pulse applied. The samples in this study were measured over a temperature range relevant to the eventual air-to-water heat exchanger, from 25 °C to 105 °C, at 10 K increments. The thermal conductivity (k) can later be directly calculated from the thermal diffusivity (α), the density (ρ), and the heat capacity (c_p) by the equation

$$k = \alpha \rho c_p \quad (\text{Eq. 2})$$

The heat capacity is measured over the relevant temperature range using a differential scanning calorimeter (DSC), DSC 214 Polyma from Netzsch Instruments (Germany).

LFA Sample Preparation

The minimum sample size for this instrument is 6 mm round, which makes the measurement 3 mm or smaller filament impossible without some additional sample preparation. Therefore, square samples with 10 mm side length with a recommended thickness around 1 mm were prepared by the techniques described below. Samples were sanded with progressively finer grains to obtain flat, level surfaces. They were then spray-coated with graphite, which aids in the absorption of the energy pulse.

In order to study the effects of filler orientation on the thermal conductivity, samples were prepared in several different ways, which are depicted below in Figure 2. The filament produced in the compounding process had three different diameters D1 (about 1.2 to 1.6 mm), D2 (about 1.7 to 2.4 mm), and D3 (about 2.5 to 3.3 mm). These were cut into 10 mm lengths, then placed lengthwise into a 10 mm by 10 mm cavity and compression molded to a height of 1 mm, 2 mm, or 3 mm. Smaller filament strands were stacked in order to fill the mold to an adequate height. Samples measured through the thickness this way demonstrate the through-plane (TP) conductivity, since the conductivity measured is perpendicular to the filament extrusion direction, which is also the dominant direction of fiber orientation.

Other samples were fabricated from the first TP samples to measure the in-plane conductivity. The 10 mm x 10 mm TP samples were cut into 1 mm strips, and each strip was

then individually rotated 90 degrees. The rotated strips were placed together in a laminate sample holder (LAM). See Figure 2 for an illustration.

Finally, another set of samples was fabricated to measure the in-plane conductivity in a different fashion. The filament produced in the compounding process, with diameters D1, D2, and D3, is cut into lengths slightly longer than 1 mm, 2 mm, or 3 mm. These are then placed standing up in the 10 mm x 10 mm mold and compression molded. The length of the filament sections was adjusted iteratively to minimize the material flow while still creating a solid sample. These in-plane compression molded (IPCM) samples also measure the in-plane conductivity. As with the other sample types, the fiber orientation may be affected by the compression.

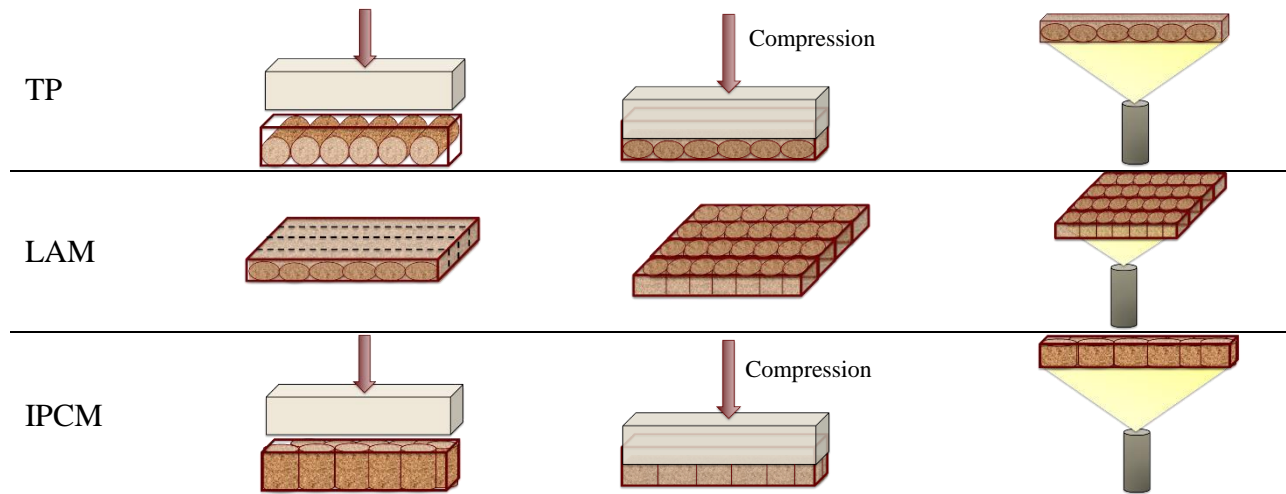


Figure 2. Sample production showing filament orientation, which is the principal fiber orientation direction. Top: through-plane (TP) samples are oriented, compressed, then scanned. Middle: in-plane laminate (LAM) samples made from TP samples by cutting and rotating strips. Bottom: in-plane compression molded (IPCM) samples are oriented, compressed, then scanned.

Micro-Computed Tomography (μ CT)

Samples were scanned with a Zeiss (Germany) Metrotom 800 μ CT scanner to analyze the fiber orientation. μ CT uses an X-ray source to take images of a sample at many different angles, and the data is subsequently reconstructed mathematically into a 3D representation of the sample. Both the filament strands produced on the twin screw extruder and the compression molded samples were analyzed. The scan resolution was 8 μ m for the filament strands, and was approximately 20 μ m for the compressed samples. This work only judges the fiber orientation qualitatively.

Results and Discussion

TGA analysis showed that all samples fell within 1 % vol of the target filler content of 20 % vol. The true filler content of each sample was then used to calculate the density of each sample for use in Eq. 2.

The specific heat capacity (c_p) was measured with DSC on the 20 % vol copper fiber material, and was found to increase linearly ($R^2 = 0.997$) from 0.95 to 1.4 kJ/kg-K over the temperature range from 25 $^{\circ}$ C to 105 $^{\circ}$ C.

Before fabricating the samples for the thermal diffusivity measurement, μ CT images of the filament were examined and are shown below in Figure 3. The spherical fillers are represented as bright points in the image. The fibers show up as fibers as well as points, which represent out of plane fibers. As expected, the fiber orientation in the extrusion direction is higher in filament of lower diameter. The fibers become more oriented in smaller filament strands due to the higher deformation in the flows; smaller cross sections cause higher shear rates which tend to orient the fibers. The fibers are less oriented in the larger diameter filament. This can be seen by the larger number of bright points, as opposed to the fiber shapes.

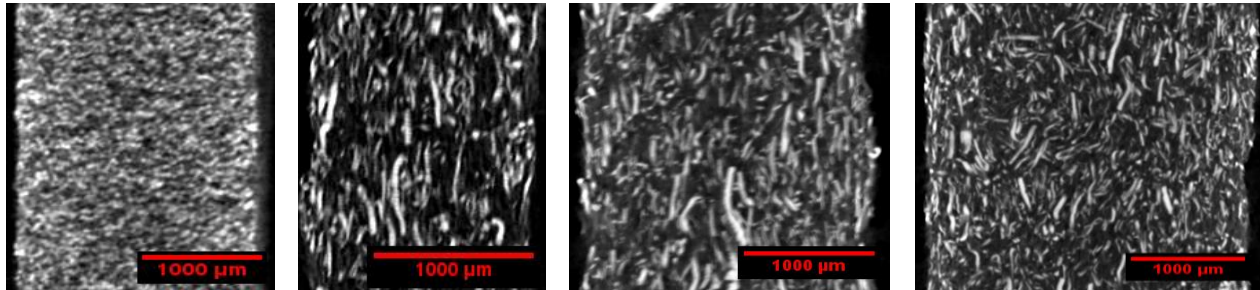


Figure 3. μ CT images of the filament strands of sizes D1, D2, and D3 produced by compounding, showing different degrees of orientation at the midplane. From left to right: D2 20% spherical filler, D1 20% fiber, D2 20% fiber, D3 20% fiber.

Thermal diffusivity was measured on several different sample types to quantify the effects of compression on the conductivity in the through-plane and in-plane directions. Sample nomenclature is as follows. D3 refers to the diameter of the filament used to create the sample. TP, IPCM, and LAM refer to the sample orientation, as explained above. 1 mm, 2 mm, or 3 mm refers to the final thickness of the sample after compression. As an example, D3-IPCM-2mm refers to a sample created with filament of approximately 3 mm in diameter, compressed in the axial direction for measuring in-plane conductivity, and the resulting compressed sample had a thickness of 2 mm.

Figure 4 shows the through-plane conductivity of samples made from 2 mm filament compressed perpendicular to the measurement and axial direction. The sample with the least compression, D2-TP-3mm, has the highest through-plane conductivity, between 1.59 and 1.63 W/m-K, which corresponds to the higher number of out of plane fibers visible in the μ CT images in Figure 3. Overall the compression ratio has no significant effect. The sample with 20 % vol copper spheres shows a significantly lower conductivity, from 0.92 to 1.01 W/m-K.

Figure 5 shows the in-plane conductivity for laminate samples (LAM), produced by cutting and rotating the samples from Figure 4, and for in-plane compressed samples (IPCM) produced by axially compressing filament in a mold. It is immediately obvious that the sample preparation methods have a large effect on the conductivity. The best performing laminate sample, D2-LAM-2mm, has a conductivity ranging from 7.04 to 7.74 W/m-K over the temperature range, while the best performing IPCM sample, D2-IPCM-3mm, ranges from 8.48 to 8.95 W/m-K. Since the fabrication method for LAM samples should tend to raise the in-plane thermal conductivity, and the method for IPCM samples should lower the in-plane conductivity, it can reasonably be expected that the true conductivity of the filament as-manufactured is somewhere between.

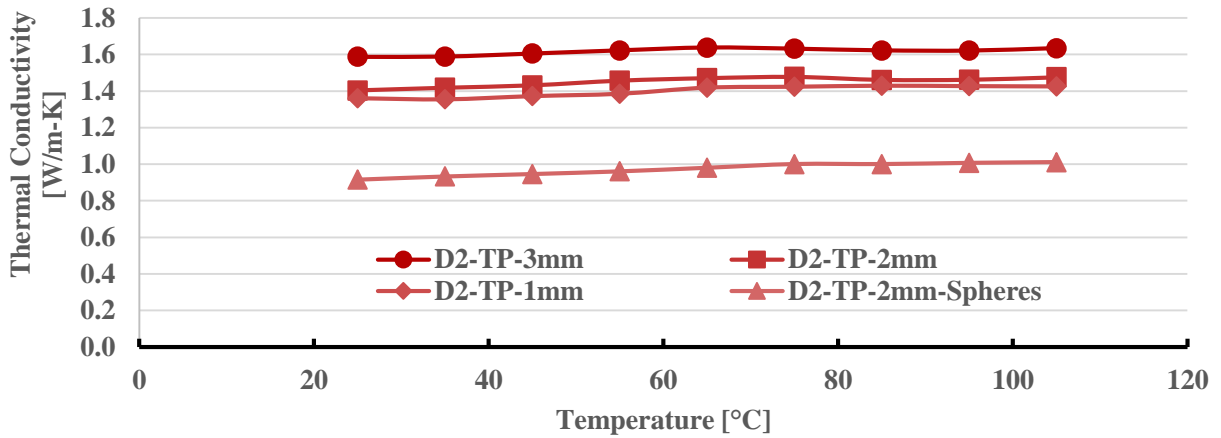


Figure 4. Through-plane conductivity in 20%vol fiber-filled samples compressed by different amounts. One sample contains 20 % vol copper spheres.

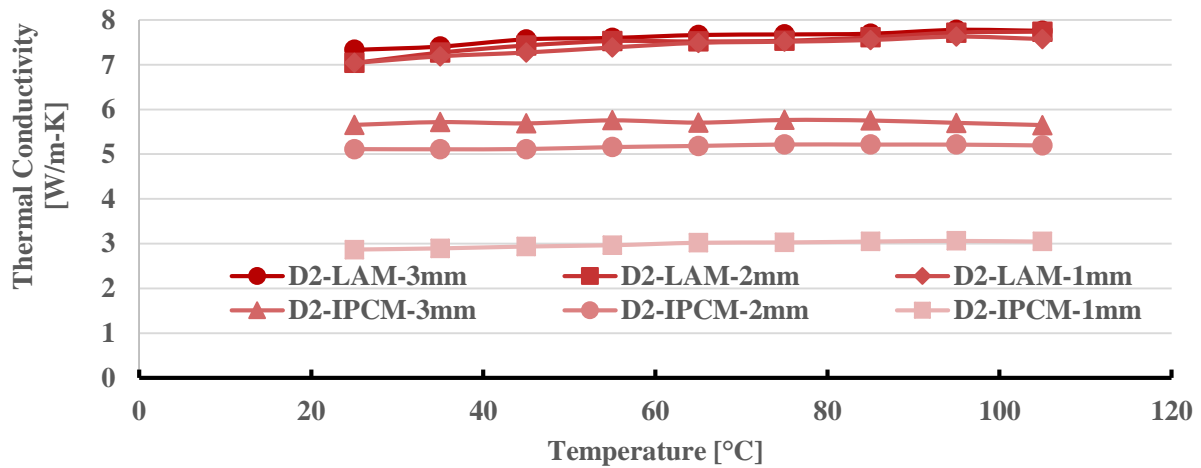


Figure 5. In-plane conductivity in 20%vol fiber-filled D2 samples fabricated differently and compressed by different amounts.

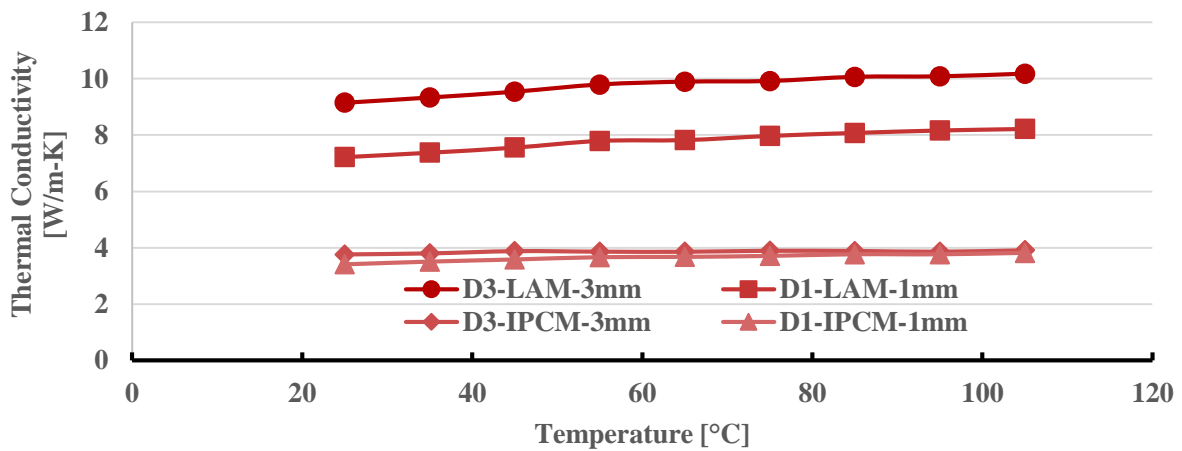


Figure 6. In-plane conductivity for LAM and IPCM samples fabricated using large (D3) or small (D1) filament with minimal compression.

Figure 6 shows the effect of different initial filament diameters on in-plane conductivity. D3-LAM-3mm is compared to D1-LAM-1mm, since both samples represent the minimum compression for those filament sizes. Similarly, D3-IPCM-3mm is compared to D1-IPCM-1mm, since both have low compression. There is very little difference in the conductivity of the IPCM samples, while the LAM samples show a difference of about 2 W/m-K. However, the conductivity of LAM samples is approximately twice as large as that of the IPCM samples.

The effects of changing fiber orientation can be clearly seen in the thermal conductivity results. The differences can also be seen in μ CT scans of the compression molded samples. Figure 7 below shows the fiber orientation in three samples made from filament of approximately 3 mm (D3) and compressed by different amounts. Since the fibers initially occupied the mold completely in the filament's axial direction, the flow during compression is mostly perpendicular to the filament axis, as the material fills in the gaps between the cylindrical surfaces. The fourth image shows a sample comprised of filament compressed axially for measurement of the in-plane properties (IPCM). In this case, the flow is again perpendicular to the filament axis, which is in the plane of the image in Figure 7. Since the majority of the fibers are still oriented with the filament axis the image below shows most of the fibers as points.

It can be generally observed that greater compression leads to a bigger change in the filament orientation. This corresponds to the thermal conductivity results discussed above.

Conclusion

Several characterization methods were explored for measuring the thermal conductivity of extruded PA6 filament with 20 % vol copper fiber or sphere fillers. It is clear from the thermal measurements, and confirmed with the μ CT scans, that the conductivity of the fiber filled samples is strongly dependent on the fiber orientation, as expected. It is shown that the sample fabrication method also strongly affects the conductivity. However, the methods were successful in characterizing the range of values for the thermal conductivity in the original filament. It is difficult to give an accurate value for the in-plane conductivity in the unaltered filament, but it should lie in the range between the in-plane compressed samples and the laminate samples, from 4 to 10 W/m-K at 25 °C. The through-plane conductivity doesn't change greatly with compression, so the true value in the filament should lie close to the measured values, approximately 3.5 W/m-K.

These values can be used for the design and simulation of the 3D-printable heat exchanger. Since the printing direction in FFF corresponds to the high in-plane conductivity, this material is advantageous for pin-type heat exchanges, since these thin structures are normally printed parallel to the pin axis. Simulations and testing are needed to determine the overall effectiveness of the heat exchanger, especially considering that the walls of the heat exchanger should correspond to the measured through-plane conductivity values. However, it is worth noting that 20 % vol fibers perform twice as well as 20 % vol spheres in the through-plane direction.

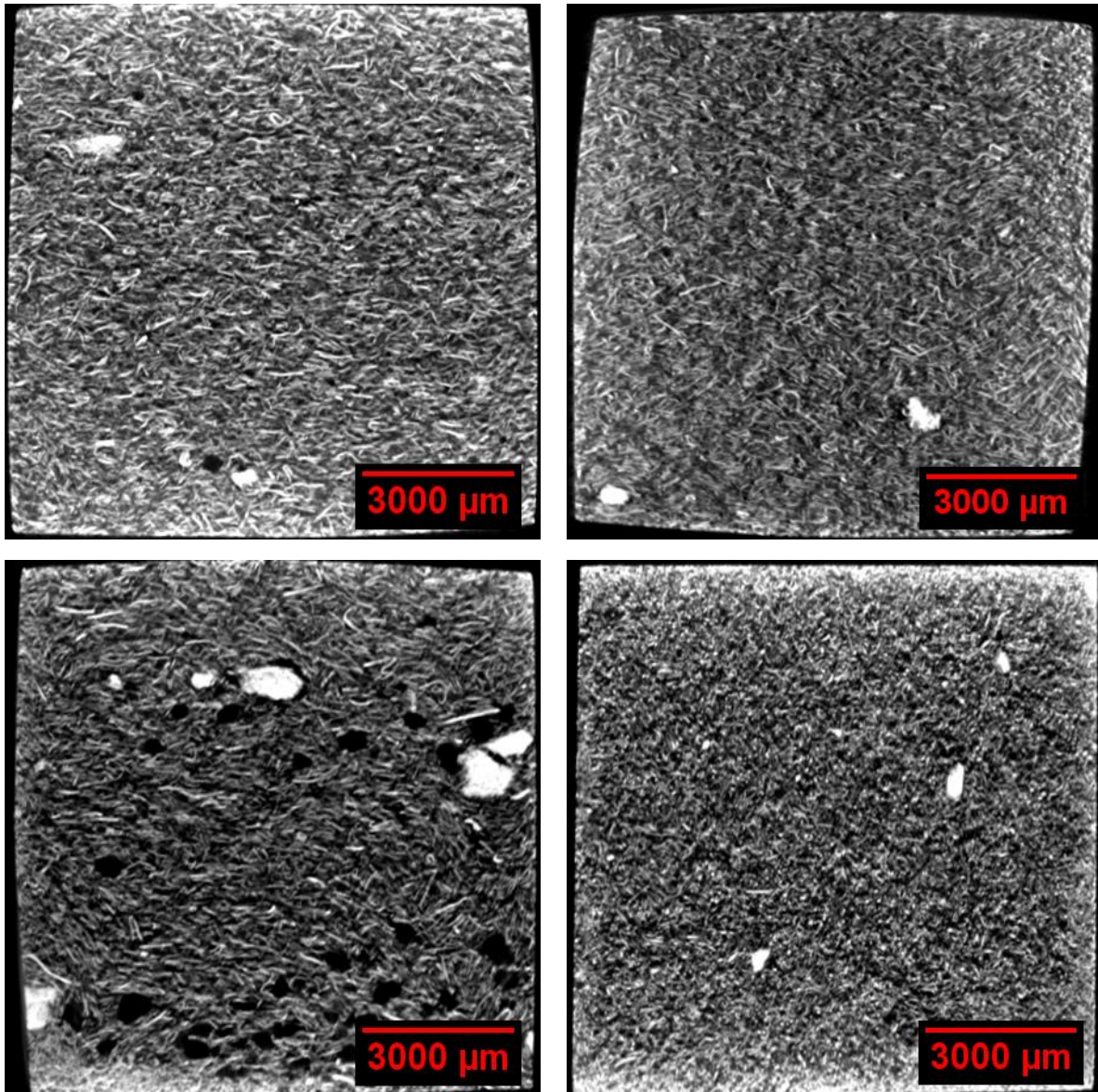


Figure 7. μ CT images showing varying degrees of orientation in compressed samples at the midplane through the thickness. Top left: D3 TP 3 mm sample, top right: D3 TP 2mm sample, bottom left: D3 TP 1 mm sample, bottom right: D3 IPCM 1 mm sample

Future Work

More tests are currently underway to compare these results with different filler volume contents. This may provide different results, considering that higher volume contents cause more fiber jamming, which leads to lower fiber orientation. Rheometry will be used to study the interaction between filler volume content and shape and the melt viscosity. The μ CT data is also being used to generate orientation matrices, which will be helpful in drawing quantitative relationships between the orientation and the thermal conductivity. These orientation matrices are derived from a method developed in-house at the Polymer Engineering Center at the University of Wisconsin – Madison [29].

Work is also ongoing on modifying traditional FFF equipment to be able to handle highly conductive materials. Possible problems may include buckling and breaking near the extruder motor, or softening there due to heat transfer from the nozzle tip along the highly conductive fiber direction. Additionally, high metallic filler content may lead to jamming and clogging of the nozzle, which could require a redesign of the nozzle geometry.

Other filler materials should also be investigated. Carbon fiber, for example, is more conductive and lightweight, which is important for mobile heat transfer applications. The materials developed through this work will be tailored for industries such as refrigeration, power electronics, and automotive.

Acknowledgements

The Polymer Engineering Center at the University of Wisconsin – Madison and the authors would like to thank BASF for material, Leistritz for the donation of the twin-screw extruder, and the U.S. Department of Energy ARPA-E for funding.

References

- [1] J. C. Riddick, M. A. Haile, R. Von Wahlde, D. P. Cole, O. Bamiduro, and T. E. Johnson, “Fractographic analysis of tensile failure of acrylonitrile-butadiene-styrene fabricated by fused deposition modeling,” *Addit. Manuf.*, vol. 11, pp. 49–59, 2016.
- [2] A. M. Kloke, “Untersuchung der Werkstoff-, Prozess- und Bauteileigenschaften beim Fused Deposition Modeling Verfahren,” Universität Paderborn, Paderborn, 2016.
- [3] I. Durgun and R. Ertan, “Experimental investigation of FDM process for improvement of mechanical properties and production cost,” *Rapid Prototyp. J.*, vol. 20, no. 3, pp. 228–235, 2014.
- [4] D. P. B. S. J. Riddick, J.C. Hall, A.J. Haile, M.A. Wahlde, R.V. Cole, “Effect of Manufacturing Parameters on Failure in Acrylonitrile–Butadiene–Styrene Fabricated by Fused Deposition Modeling,” *Struct. Dyn. Mater. Conf.*, vol. 53, no. April, pp. 1–8, 2012.
- [5] K. Kirchner, H. Jäschke, H.-J. Franke, T. Vietor, and K.-H. Grote, “Mechanisch-technologische Eigenschaften generativ gefertigter Bauteile in Abhängigkeit von der Bauteilorientierung,” *RTEjournal*, pp. 1–8, 2010.
- [6] A. K. Sood, R. K. Ohdar, and S. S. Mahapatra, “Improving dimensional accuracy of Fused Deposition Modelling processed part using grey Taguchi method,” *Mater. Des.*, vol. 30, no. 10, pp. 4243–4252, 2009.
- [7] A. Bellini and S. Güçeri, “Mechanical characterization of parts fabricated using fused deposition modeling,” *Rapid Prototyp. J.*, vol. 9, no. 4, pp. 252–264, 2003.

- [8] M. Bertoldi, M. a Yardimci, C. M. Pistor, S. I. Guceri, and G. Sala, “Mechanical characterization of parts processed via fused deposition,” *Solid Free. Fabr. Proc.*, pp. 557–565, 1998.
- [9] L. Li, Q. Sun, C. Bellehumeur, and P. Gu, “Composite Modeling and Analysis for Fabrication of FDM Prototypes with Locally Controlled Properties,” *J. Manuf. Process.*, vol. 4, no. 2, pp. 129–141, 2002.
- [10] M. Montero, S. Roundy, and D. Odell, “Material characterization of fused deposition modeling (FDM) ABS by designed experiments,” *Proc. Rapid Prototyp. Manuf. Conf.*, pp. 1–21, 2001.
- [11] J. F. Rodríguez, J. P. Thomas, and J. E. Renaud, “Mechanical behavior of acrylonitrile butadiene styrene fused deposition materials modeling,” *Rapid Prototyp. J.*, vol. 7, no. 3, pp. 148–158, 2001.
- [12] O. S. Es-Said, J. Foyos, R. Noorani, M. Mendelson, R. Marloth, and B. A. Pregger, “Materials and Manufacturing Processes Effect of Layer Orientation on Mechanical Properties of Rapid Prototyped Samples Effect of Layer Orientation on Mechanical Properties of Rapid Prototyped Samples,” *Mater. Manuf. Process.*, vol. 15, no. 1, pp. 107–122, 2000.
- [13] S.-H. Ahn, M. Montero, D. Odell, S. Roundy, and P. K. Wright, “Anisotropic material properties of fused deposition modeling ABS,” *Rapid Prototyp. J.*, vol. 8, no. 4, pp. 248–257, 2002.
- [14] Pfeifer, Thomas, Koch, Carsten, Van Hulle, Luke, Mazzei Capote, Gerardo. “Optimization of the FDM additive manufacturing process. Proceedings of SPE ANTEC 2016.
- [15] Amesöder, Simon. Wärmeleitende Kunststoffe für das Spritzgießen, PhD thesis, University of Erlangen-Nuremberg, 2010.
- [16] Heinle C., Simulationsgestützte Entwicklung von Bauteilen aus wärmeleitfähigen Kunststoffen, PhD thesis, University of Erlangen-Nuremberg, 2013.
- [17] Tsekmes, I.A., Kochetov, R., Morshuis, P.H.F., Smit, J.J. “Thermal conductivity of polymeric composites: a review.” 2013 IEEE International Conference on Solid Dielectrics, Bologna, Italy, 2013.
- [18] Gray R.W., Baird D.G., Bohn J.H., Effects of processing conditions on short TLCP fiber reinforced FDM parts, *Rapid Prototyping Journal*, vol. 4, no. 1, pp.14–25, 1998.
- [19] Gray R.W., Baird D.G., Bohn J.H., Thermoplastic composites reinforced with long fiber thermotropic liquid crystalline polymers for fused deposition modeling, *Polymer Composites*, vol.19, no. 4, pp. 383–394, 1998.

- [20] Zhong W., Li F., Zhang Z., Song L., Li Z., Short fiber reinforced composites for fused deposition modeling, *Materials Science and Engineering*, A301, pp. 125–130, 2001.
- [21] Masood S.H., Song W.Q., Development of new metal/polymer materials for rapid tooling using fused deposition modeling, *Materials and Design*, vol. 25, pp. 587–594, 2004.
- [22] Nikzad M., Masood S.H., Sbarski L., Thermo-mechanical properties of highly filled polymeric composites for fused deposition modeling, *Materials and Design*, vol. 32, pp. 3448–3456, 2011.
- [23] Leigh SJ, Bradley RJ, Purssell CP, Billson DR, Hutchins DA, A Simple, Low-Cost Conductive Composite Material for 3D Printing of Electronic Sensors, *PLOS ONE* 7(11): e49365, 2012, doi:10.1371/journal.pone.0049365
- [24] ORNL demonstrates 3-D printing with carbon fiber, *Composites World*, June, 2014, *Composite Science and Technology*, 105 (2014), pp.144-150.
<http://www.compositesworld.com/blog/post/ornl-demonstrates-3-d-printing-with-carbon-fiber>
- [25] Tekinalp, H., Kunc, V., Velez-Garcia, G., Duty, C., Love, L., Naskar, A., Blue, C. and Ozcan, S., Highly oriented carbon fiber-polymer composites via additive manufacturing, *Composites Science and Technology*, vol. 105, pp. 144-150, 2014.
- [26] Ferber, Rachel, Rudolph, Natalie, and Nellis, Gregory. “Design and simulation of 3D printed air-cooled heat exchangers.” *Proceedings of Solid Freeform Fabrication Symposium*, 2016.
- [27] Parker, W.J., Jenkins, R.J., Butler, C.P., Abbott, G.L. “Flash method of determining thermal diffusivity, heat capacity, and thermal conductivity.” *J. App Physics*, vol. 32, p. 1679, 1961.
- [28] Cowan, Robert. “Pulse method of measuring thermal diffusivity at high temperatures.” *J App Physics*, vol. 34, p. 926, 1963.
- [29] Goris, S., Fontana, C., Osswald, T. “Fiber orientation measurements using a novel image processing algorithm for micro-computed tomography scans.” *Proceedings of SPE ANTEC* 2015.